

Glutamate modulates the firing rate in oculomotor nucleus motoneurons as a function of the recruitment threshold current

Julio Torres-Torrel, David Rodríguez-Rosell, Pedro Nunez-Abades, Livia Carrascal and Blas Torres

Department of Physiology, University of Seville, Seville, Spain

Key points

- This study deals with the cellular mechanisms involved in firing rate modulation *in vivo* in the oculomotor system where there are requirements for high firing rates by motoneurons.
- The study demonstrates that glutamate effects depend on the recruitment threshold and, presumably, motoneuron size.
- Mid- and high-threshold motoneurons in response to glutamate decrease their voltage threshold and strengthened the tonic and phasic components of the firing rate.
- In a functional context, motoneurons could be recruited at lower recruitment threshold and could generate a strong muscle contraction under glutamate modulation to perform saccadic eye movements with different velocities and/or to maintain the eye in different eccentric positions in the orbit.
- Our results suggest that the recruitment and firing behaviour of ocular motoneurons can be modified *in vivo* by glutamatergic synaptic inputs. It provides a link between cellular function and behavioural motoneuron output.

Abstract Studies in alert preparations have demonstrated that ocular motoneurons exhibit a phasic–tonic firing rate related to eye velocity and position, respectively. The slopes of these relationships are higher in motoneurons with higher recruitment threshold and have been proposed to depend upon synaptic input. To investigate this hypothesis, motoneurons of the rat oculomotor nucleus were recorded in a brain slice preparation in control conditions and during glutamate ($5 \mu\text{M}$) application to the bath. Glutamate did not affect membrane potential or input resistance, but produced a decrease in rheobase and depolarization voltage as a function of the current needed for generating a maintained repetitive discharge (recruitment threshold current). In addition, glutamate compressed the range of recruitment threshold current ($0.1\text{--}0.4 \text{ nA}$) as compared to the control ($0.15\text{--}0.7 \text{ nA}$). Glutamate exposed motoneurons showed an increase in the tonic frequency gain and the peak frequency. Such increments depended on the recruitment threshold current and the last recruited motoneurons almost doubled the tonic frequency gain (35.2 vs. $57.9 \text{ spikes s}^{-1} \text{ nA}^{-1}$) and the peak frequency (52.4 vs. $102.6 \text{ spikes s}^{-1}$). Finally, glutamate increased the spike frequency adaptation due to a significant increase in the phasic firing component as compared to the tonic one. In conclusion, glutamate modulates tonic and phasic discharge properties as a function of the recruitment threshold current and, presumably, motoneuron size. These findings contribute to understand the link between cellular functions and motoneuron discharge during oculomotor behaviour.

(Received 21 December 2011; accepted after revision 1 May 2012; first published online 8 May 2012)

Corresponding author B. Torres: Dept. Fisiología, Fac. Biología, Avenida Reina Mercedes, 6, 41012 Sevilla, Spain.
Email: btorres@us.es

J. Torres-Torrel and D. Rodríguez-Rosell contributed equally to this work.

Introduction

Glutamate is the major excitatory neurotransmitter in the nervous system. Based on immunohistochemical procedures, neurons that use aspartate and/or glutamate as neurotransmitters have been reported to project towards the oculomotor nucleus from different visuomotor and vestibular brainstem sources (Kevetter & Hoffman, 1991; Carpenter, 1992; Spencer & Wang, 1996; Nguyen & Spencer, 1999; Nguyen *et al.* 1999). In addition, ionotropic and metabotropic glutamate receptors have been identified within the oculomotor nucleus by measuring the expression of different subunits (Laslo *et al.* 2001a,b; Fuller *et al.* 2006; Hideyama *et al.* 2010). In abducens motoneurons recorded *in vivo*, the activation of glutamate receptors does not produce any change in input resistance, and induces a small membrane potential depolarization that does not bring the motoneuron to fire (Durand *et al.* 1987). However, selective activation of ionotropic glutamate receptors has been consistently shown to induce an increase in input resistance, and a depolarization in the membrane potential that evokes repetitive firing (Durand, 1991, 1993; Ourdouz & Durand, 1994; Ruiz & Durand, 1999).

Qualitatively, all ocular motoneurons discharge in a tonic–phasic manner related to eye position and eye velocity, respectively. The firing rates of ocular motoneurons in relation to steady-state eye positions have been measured in a number of species (Delgado-García *et al.* 1986; Fuchs *et al.* 1988; de la Cruz *et al.* 1989; Pastor *et al.* 1991; Stahl & Simpson, 1995; Sylvestre & Cullen, 1999; Davis-López de Carrizosa *et al.* 2011). An individual motoneuron begins to fire when the position of the eye reaches a certain threshold position in the pulling direction of the muscle that the motoneuron innervates (on-direction). Above this threshold, the motoneuron exhibits a tonic discharge whose rate increases linearly with more eccentric eye positions in the on-direction. The slope of this relationship (termed k) indicates eye position sensitivity. The recruitment threshold and k vary across motoneurons, with distribution over a large range that ensures a fine gradation of force and stable eye position. Besides, recruitment threshold and k are positively correlated: motoneurons with higher threshold also have steeper slopes k . Results obtained *in vitro* suggest that synaptic inputs play an important role in determining the relationship between the recruitment threshold and the tonic firing rate (Nieto-Gonzalez *et al.* 2007, 2009). This suggestion is consistent with the evidence provided by simulation studies (Dean, 1997; Hazel *et al.* 2002) and after deafferentation of motoneurons (Pastor & González-Forero, 2003). The first aim of this work was to determine *in vitro* if the relationship between eye position sensitivity and recruitment threshold reported *in vivo* could be set by the activation of glutamatergic receptors.

Ocular motoneurons also exhibit a burst of spikes (phasic component of the firing) that co-varies with saccade velocity in the on-direction. In addition, it is well known that peak firing rate is strongly related to peak eye velocity during saccades (Delgado-García *et al.* 1986; Gomez *et al.* 1986). The slope of the relationship between phasic firing and eye velocity is termed r and indicates the eye velocity sensitivity of each motoneuron. Furthermore, motoneurons with higher threshold also tend to exhibit higher sensitivity to eye velocity (Davis-López de Carrizosa *et al.* 2011). *In vitro* studies carried out in the oculomotor and trochlear nuclei of rats and turtle have reported two types of motoneurons: the first type shows an essentially tonic firing rate (with a weak phasic component), while the second type has a phasic–tonic discharge. The phasic component was more pronounced in the second type of motoneurons (Nieto-Gonzalez *et al.* 2007; Jones & Ariel, 2008). These two types of motoneurons are likely to be part of a functional continuum rather than two separate populations (Nieto-Gonzalez *et al.* 2007). The significance of motoneurons with different phasic responses raises the possibility that they may be determined by their synaptic inputs. Taking into account these findings, high recruitment threshold motoneurons may receive a more powerful source of phasic synaptic inputs than low-threshold motoneurons, as proposed in spinal motoneurons (Powers *et al.* 1993). Thus, the second aim of this work was to test whether the effects of the glutamatergic activation on the phasic responses were related to motoneuron thresholds.

Methods

Surgery and solutions

Experiments were carried out in young Wistar rats, 15–25 days old, of both sexes. The experiments were performed in accordance with the European Community Directive 2003/65, as well as with the Spanish Royal Decree 120/2005 and University of Seville regulations on the care and use of laboratory animals. Rats were deeply anaesthetized with sodium pentobarbital (50 mg kg⁻¹) and quickly decapitated. The methods to obtain the slices, recordings and analysis are fully detailed in previous studies (Carrascal *et al.* 2006; Nieto-Gonzalez *et al.* 2009). In brief, brain slices of 300 μ m including the oculomotor nucleus were first incubated in a chamber containing cold sucrose-artificial cerebrospinal fluid (ACSF) for 20–30 min, and then transferred to a second chamber containing ACSF at a temperature of $21 \pm 1^\circ\text{C}$. Single slices were transferred to the recording chamber and superfused at 2 ml min⁻¹ (Harvard, MPIO, Holliston, Massachusetts, USA) with ACSF bubbled with 95% O₂–5% CO₂ (pH 7.4; 32°C). The composition of ACSF was as follows (in mM): 126 NaCl, 2 KCl, 1.25 Na₂HPO₄,

26 NaHCO₃, 10 glucose, 2 MgSO₄, and 2 CaCl₂. For sucrose-ACSF solution, the NaCl was replaced by sucrose (240 mM). Glutamate (L-glutamic acid, Sigma-Aldrich) was dissolved in distilled water for stock solution (10 mM) and stored frozen at -20°C. Glutamate was diluted in the ACSF at 5 μM for the experiments. The experiment included the recording of the same motoneuron before (control) and during glutamate exposure (glutamate condition). After recordings in the control condition, the slices were superfused with glutamate at 2 ml min⁻¹ (pH 7.4; 32°C, TC-324B Warner Instruments), and 3–4 min later the recordings were performed. The time taken to completely exchange ACSF solution for glutamate solution was about 50 s. One motoneuron per slice was recorded.

Electrophysiological recordings and data analysis

All recorded neurons were identified as motoneurons by their antidromic activation from the root of the third nerve and by the collision test (Carrascal *et al.* 2006). The recordings were carried out with sharp microelectrodes that were filled with a 3 M KCl (30–60 MΩ) solution. Recordings were stored on videotape (Neuro-Corder, Neurodata Instruments, PA, USA), and subsequently played back and acquired with a PCI-6070E card (National Instruments, Austin, TX, USA) for off-line analysis. All motoneurons included for analysis showed a stable resting membrane potential of at least -55 mV, an action potential amplitude greater than 60 mV, and fired repetitively in response to supra-threshold depolarizing current steps of 1 s. The bridge balance was routinely monitored and adjusted before any cell impalement. The bridge balance removed most of the component of voltage (increases in voltage amplitude were lower than 3 mV) and voltage rectification was small (less than 1 mV) for injected currents up to 1 nA. In addition, the stability in membrane potential along with input resistance, rheobase and action potential features were systematically measured at periodic intervals throughout the recording period to assess the quality of the impalement. Recordings with deterioration in these physiological properties were discarded. Resting membrane potentials were measured as the difference between the intracellular and extracellular potentials after withdrawing the recording electrode from the cell. The input resistance was determined by passing negative current pulses (500 ms, 1 Hz; with 0.1 nA increments). Input resistance was calculated as the slope of the current–voltage plot. The rheobase was the minimum current injected (50 ms, 1 Hz) that generated action potentials in 50% of the cases. The depolarization voltage was the increment in membrane potential required to bring the cell to the spike threshold. To determine the spike threshold, the action potential recording was differentiated; spike onset was the value of the membrane

potential at which the first derivative exceeded 10 V s⁻¹. The voltage threshold to elicit a single action potential was calculated by adding depolarization voltage to the resting membrane potential. The tonic component of the firing was measured from the repetitive discharge evoked by depolarizing current steps (1 s, 0.5 Hz) with 0.05 nA increments. The steady-state firing frequency was the average number of spikes during the last 500 ms. The relationship between the steady-state firing frequency and injected current was represented (*I–F* plot) to calculate the slope, namely as tonic frequency gain. The recruitment threshold current was defined as the lowest intensity of stimulating current capable of eliciting a maintained repetitive firing (Kernell *et al.* 1999). The variability of repetitive firing was measured in the interspike intervals at different firing rates evoked by different current intensities for each motoneurons. The coefficient of variation (standard variation/mean duration × 100) of the interspike interval of each firing rate was plotted against current intensity. The data were fitted with two regression lines, one for data that showed low firing variability and the other when firing variability was high. The recruitment threshold current was taken as the current step (with low firing variability) closest to the point at which the regression lines intersected. The minimal steady-state firing rate was that associated to the recruitment threshold current (for details, of the relationship between firing variability and threshold, see Piotrkiewicz *et al.* 1999, Powers & Binder, 2000; González-Forero *et al.* 2002). This procedure was carried out in motoneurons that exhibited a progressive increase in firing rate as a function of the stimulating current intensity. However, some motoneurons exhibited a sudden transition from sub-threshold to maintained repetitive firing. In these cases, the recruitment threshold current was the lowest stimulating current capable of eliciting a maintained repetitive firing with a coefficient of variation ≤10% (motoneurons with a progressive increase in firing rate exhibited a point of intersection between lines of low and high firing variability at coefficient of variation ≤10%). The phasic component of the firing was calculated by measuring the peak frequency, which corresponded to the reciprocal of the time interval between the two first spikes, at a current capable of eliciting 20 spikes s⁻¹ of tonic discharge (a frequency at which all motoneurons showed a steady-state firing rate). In addition, we measured the spike frequency adaptation according to the *initial* adaptation index (Sawczuk *et al.* 1995; Rekling *et al.* 2000), calculated as [1 – (frequency in the steady-state firing/instantaneous frequency in the first interspike interval)]. The adaptation process calculated from this equation generated values between 0 and 1, the values 0 or 1 being pure tonic or phasic responses, respectively. The change in all studied parameters was normalized and measured as the value of the parameter in the glutamate condition/the value in the control

condition. Such changes were plotted against recruitment threshold current. Significant differences between control and glutamate conditions were determined by using Student's paired *t* test. The correlation between variables was measured by Pearson's correlation coefficient (*r*). The significance level was established at *P* < 0.05. All data are reported as means \pm standard error of the mean.

Results

Membrane potential and input resistance responses to glutamate exposure

All recorded motoneurons (*n* = 33) of the oculomotor nucleus were silent at their resting membrane

potential (-61.3 ± 1.5 mV), and required supra-threshold depolarizing current steps to evoke a phasic-tonic firing. The electrophysiological effects of glutamate were reversed when slices were washed with ACSF solution for 20 min. Glutamate superfusion induced a very small, if any, membrane potential depolarization (<5 mV; Fig. 1A). The injection of negative current pulses produced a membrane hyperpolarization. In response to equal current steps, the amplitude of the hyperpolarization was similar between the control and glutamate conditions (Fig. 1B). The plot of current pulses against voltage generated a linear fit, and the slopes of these relationships indicated the input resistance (Fig. 1C). Input resistance did not change with glutamate application (control = 57.3 ± 4.2 M Ω ; glutamate = 56.7 ± 4.0 M Ω ; Fig. 1D).

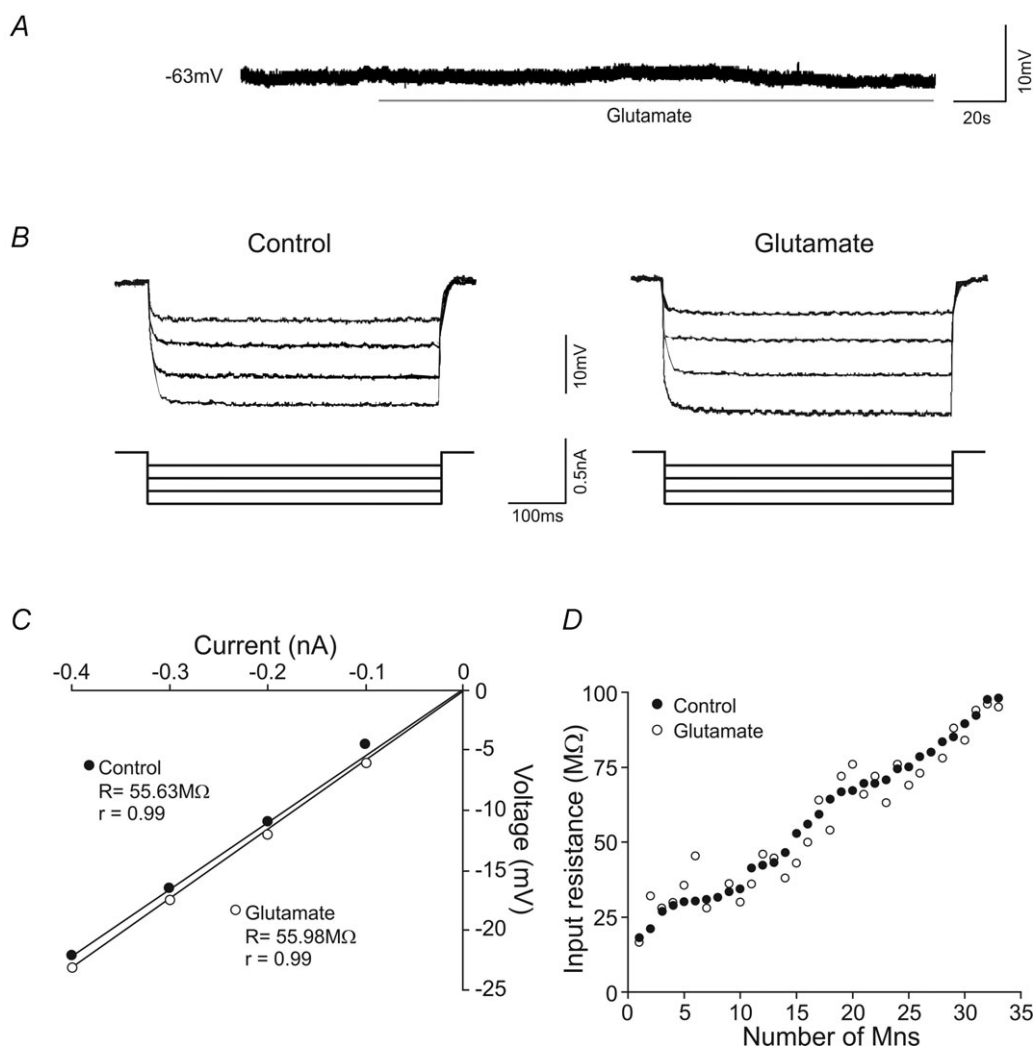


Figure 1. Effects of glutamate on membrane potential and input resistance

A, membrane potential response to glutamate exposure. B, responses of the membrane potential to hyperpolarizing current pulses of the same intensities in control and glutamate conditions. C, plot illustrating the current/voltage relationships to determine the input resistance (*R*) for the motoneuron illustrated in B. D, plot illustrating the value of input resistance for each motoneuron in control and glutamate conditions. All analysed motoneurons are represented and arranged as a function of their input resistance.

Rheobase and depolarization voltage responses to glutamate exposure

The motoneurons exposed to glutamate showed a decrease in rheobase and depolarization voltage (Fig. 2). Figure 2*A* and *B* illustrates the same motoneuron in the control (*A*) and glutamate (*B*) conditions. The motoneuron maintained its membrane potential (-62 mV) and input resistance (56 vs. 60 M Ω), but both rheobase (0.3 vs. 0.1 nA) and depolarization voltage (16.8 vs. 6 mV) decreased. The diminution in depolarization voltage while the membrane potential remained at rest involved a decrease in voltage threshold (-45.2 vs. -56 mV) with drug treatment. These findings are consistent with those obtained from all of motoneurons analysed. Thus, the rheobase (0.27 ± 0.03 vs. 0.19 ± 0.03 nA) and depolarization voltage (16.25 ± 1.1 vs. 12.5 ± 1.3 mV)

decreased with the exposure to glutamate. Although glutamate had little effect on input resistance or resting potential as a whole, we examined whether these factors contributed to the effects of glutamate on the rheobase and depolarization voltage. Rheobase and voltage depolarization changes (before and during glutamate application) were not correlated with either membrane potential or input resistance changes. On the other hand, glutamate application yielded a left-ward shift in rheobase and voltage depolarization when the data were plotted in cumulative normalized diagrams (Fig. 2*C* and *D*). According to these plots, in the control condition 50% of motoneurons fired with rheobase values ≤ 0.26 nA and with depolarization voltage ≤ 17 mV; in the glutamate condition 50% of motoneurons fired with rheobase ≤ 0.16 nA and with depolarization voltage ≤ 12 mV.

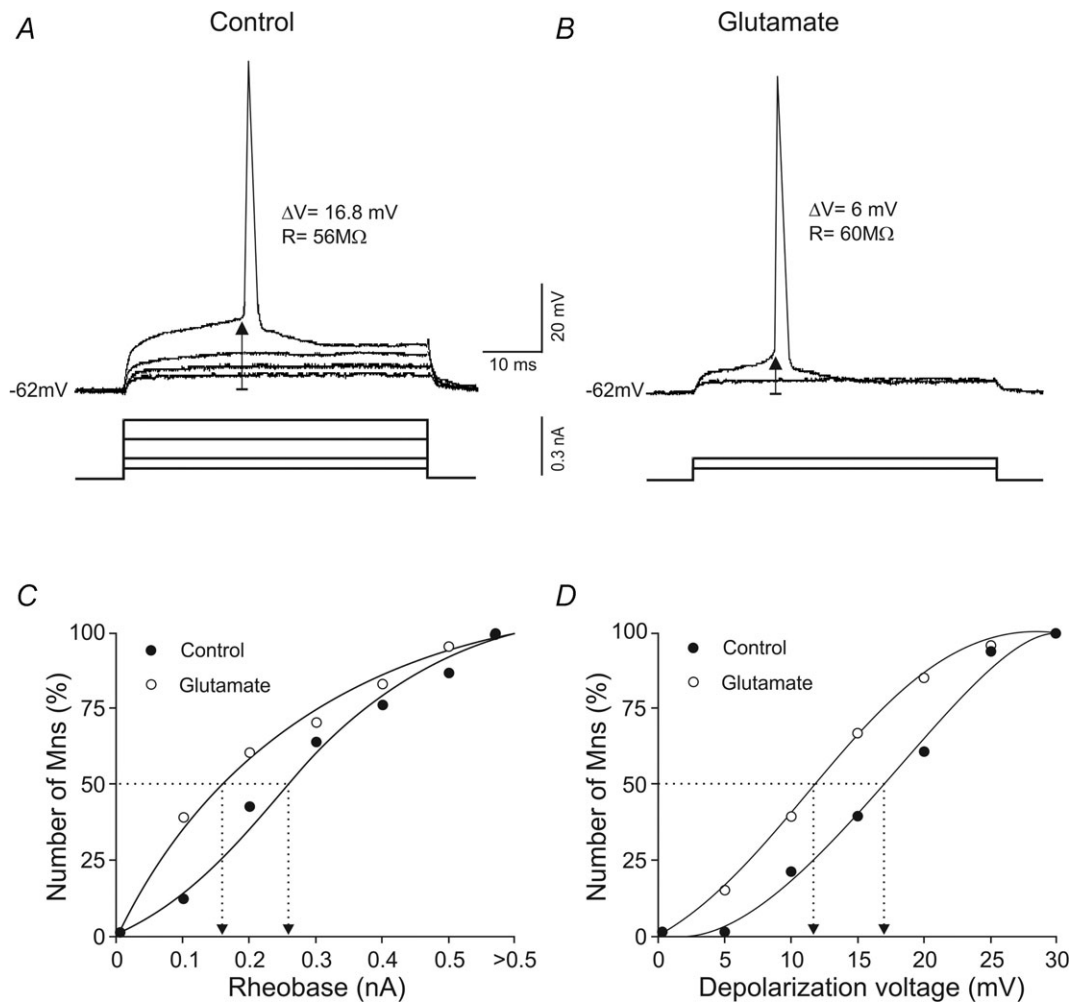


Figure 2. Effects of glutamate on rheobase and depolarization voltage

A and *B*, recordings showing the minimum current (rheobase) and voltage depolarization required to evoke an action potential in the same motoneuron in control and glutamate conditions. ΔV and R indicate depolarization voltage and input resistance, respectively. *C* and *D*, cumulative normalized plots of rheobase and depolarization voltage in control and glutamate conditions. The dotted lines show the rheobase and depolarization values at which 50% of the motoneurons evoked an action potential.

The previous findings demonstrate that glutamate treatment diminished the values of rheobase and depolarization voltage in the oculomotor nucleus motoneurons. We next studied if these effects depended on the recruitment threshold current. Figure 3A–C, illustrates three motoneurons with different recruitment thresholds: low (Fig. 3A), mid (Fig. 3B) and high (Fig. 3C). In the control condition, these motoneurons exhibited a similar resting membrane potential close to -62 mV, but different rheobase and depolarization voltage. Bath application of glutamate modified neither the resting membrane potential nor the input resistance, but yielded a decrease in rheobase and depolarization voltage in both mid- and high-threshold motoneurons. As shown in the figure, the magnitudes of decreases in rheobase and in depolarization voltage were more pronounced in the high-threshold motoneurons. This observation was further documented when changes in both rheobase and depolarization voltage were plotted against recruitment threshold current (Fig. 3D and E). Both parameters were linearly related to recruitment threshold current,

and the last recruited motoneurons exhibited the most pronounced changes in both rheobase and depolarization voltage.

Tonic firing rate response to glutamate exposure

In response to supra-threshold depolarizing current steps, motoneurons exhibited a phasic–tonic discharge rate. The tonic component of the firing produced by equal depolarizing current steps in control and glutamate conditions was measured. As shown in Fig. 4A and B, the number of spikes was higher when the motoneuron was exposed to glutamate. Neither resting membrane potential nor input resistance changed in the glutamate condition, but in response to current steps of 0.25 and 0.5 nA, the motoneuron discharged 4 and 14 spikes s^{-1} , respectively, in the control condition and 14 and 30 spikes s^{-1} , respectively, when treated with glutamate. The recruitment threshold current and steady-state firing rate was calculated for each motoneuron. For the representative example illustrated

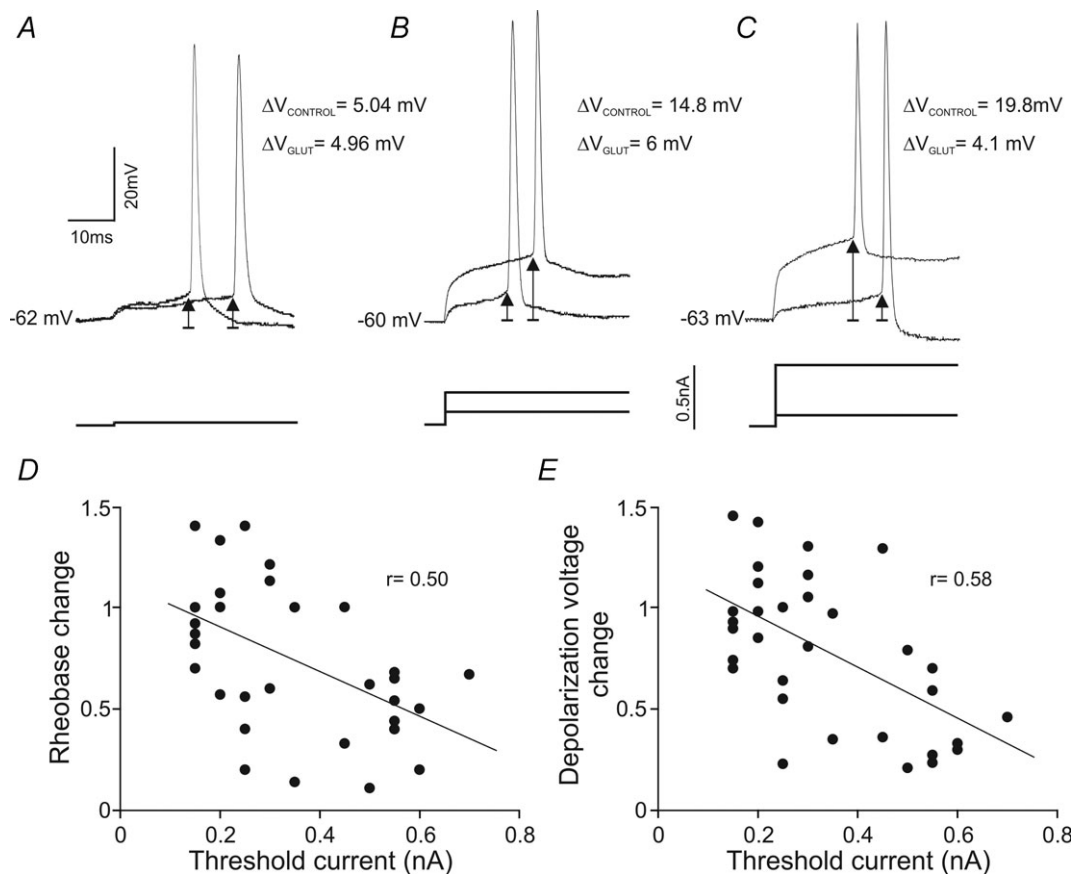


Figure 3. Effects of glutamate on rheobase and depolarization voltage as a function of the recruitment threshold

A–C, three representative motoneurons with low- (A), mid- (B) and high- (C) threshold recorded in control and glutamate conditions. ΔV indicates depolarization voltage. D and E, plots illustrating the change in both rheobase and depolarization voltage as a function of the recruitment threshold current.

in Fig. 4C, the recruitment threshold current was 0.45 and 0.25 nA in control and glutamate conditions, respectively, and the minimal steady-state firing rate was 15 and 14 spikes s⁻¹ nA⁻¹ in control and glutamate conditions, respectively. The *I*-*F* plots in both conditions showed a linear relationship (*r* = 0.99) in all studied motoneurons, and the slope of these relationships was termed tonic frequency gain. For the motoneuron represented in Fig. 4A

and B, glutamate treatment evoked the following: first, a higher tonic frequency gain; second, a decrease in the recruitment threshold current; and third, a higher tonic firing frequency throughout the whole range of current stimulation (Fig. 4D).

Figure 5A and B shows *I*-*F* relationships of all studied motoneurons. In the control condition, the motoneurons exhibited a tonic frequency gain that ranged from

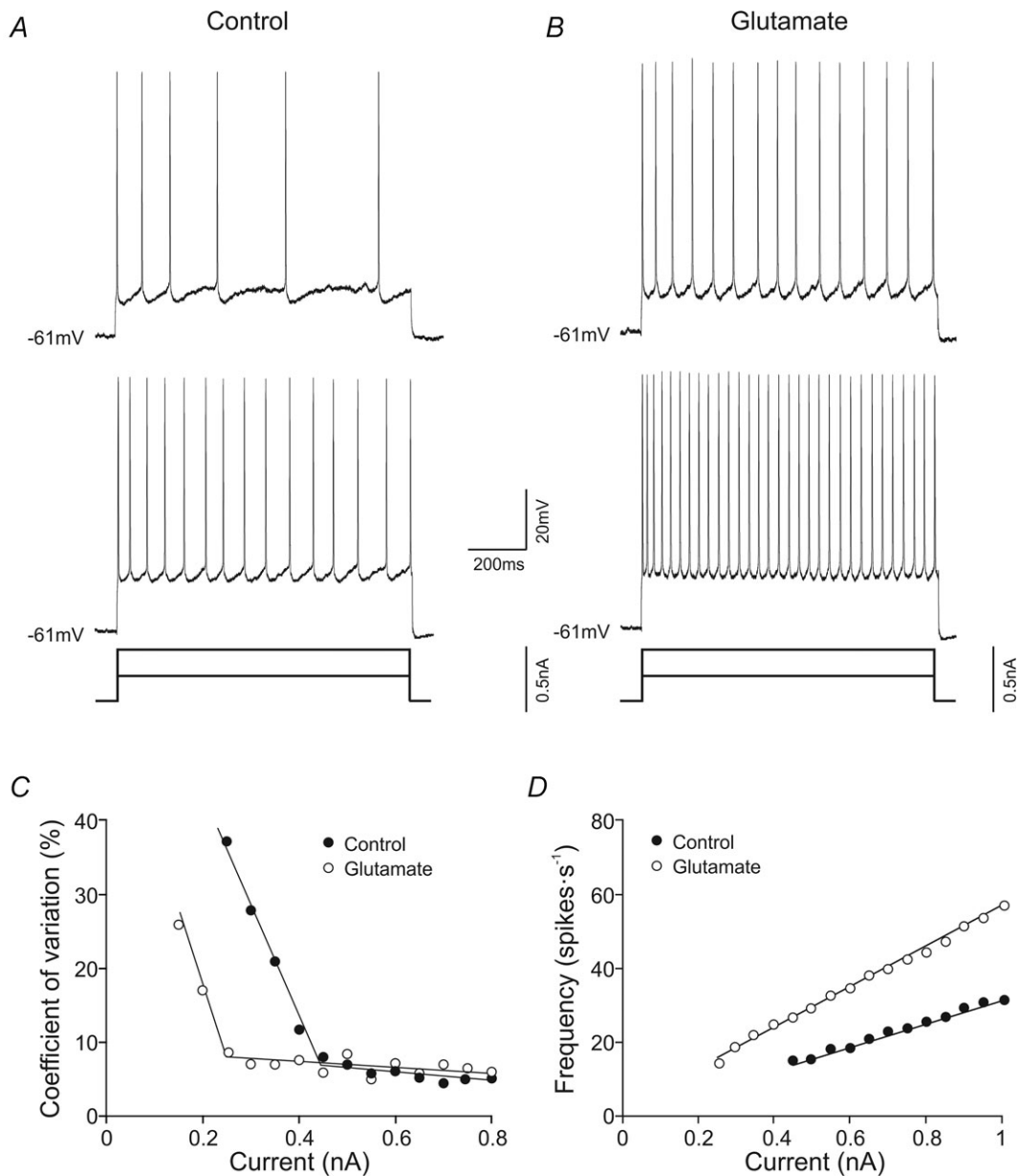


Figure 4. Effects of glutamate on tonic frequency gain
 A and B, firing discharge of a high-recruitment current motoneuron in response to two different current steps in control (A) and glutamate (B) conditions. C, plot illustrating the relation between the coefficient of variation of the interspike intervals measured at different firing rates and stimulating current intensities. D, plots of the steady-state frequency against current intensity (*I*-*F* plots) for a motoneuron in control (C) and glutamate (D) conditions. It should be noted that this motoneuron showed an increase in tonic frequency gain and a decrease in recruitment threshold current in the glutamate condition.

17.3 to 98.6 spikes s^{-1} nA^{-1} (47.7 ± 2.9 spikes s^{-1} nA^{-1}), and in the glutamate condition it ranged from 26.6 to 132.3 spikes s^{-1} nA^{-1} (58.4 ± 3.5 spikes s^{-1} nA^{-1}). In the control condition the recruitment threshold current ranged from 0.15 to 0.7 nA (0.35 ± 0.03 nA), and was compressed in glutamate-exposed motoneurons to values ranging from 0.1 to 0.4 nA (0.24 ± 0.01 nA). In addition, the minimal repetitive firing rate was 15.2 ± 0.37 spikes s^{-1} nA^{-1} in control condition and 13.6 ± 0.28 spikes s^{-1} nA^{-1} during glutamate application to the bath. The glutamate treatment decreased the recruitment threshold current in some motoneurons, but such a decrease was different from one motoneuron to another. Indeed, both parameters (recruitment threshold current change and recruitment threshold current) were linearly related, with the most pronounced changes in the last recruited motoneurons (Fig. 5C). The glutamate effect in tonic frequency gain was also different from one motoneuron to another. Changes in tonic frequency gain ranged from 0.8 to 2.4. Furthermore, the changes in tonic frequency gain increased linearly with the recruitment threshold current (Fig. 5D). This positive co-variation indicates that the last recruited motoneurons were those more sensitive to glutamate exposure, i.e. when the tonic frequency gain showed a more pronounced increase

(up to 2.4-fold). Thus, motoneurons with recruitment threshold current higher than 0.5 nA exhibited a tonic frequency gain of 35.2 ± 3.8 spikes s^{-1} nA^{-1} in control condition, while it was 57.9 ± 6.2 spikes s^{-1} nA^{-1} when exposed to glutamate. In addition, some motoneurons with a low recruitment threshold current (4/33) exhibited a slight decrease in gain (between 0.8–1).

We also analysed if the recruitment threshold current co-varied with input resistance (Fig. 6). A significant linear relationship was found between these two parameters in the control condition (Fig. 6A). According to this relationship, motoneurons with higher input resistance showed lower recruitment threshold current to evoke a repetitive discharge. However, no significant relationship between the recruitment threshold current and input resistance was found in the glutamate condition (Fig. 6B). This lack of relationship was due to the following: first, input resistance was essentially unaltered with glutamate exposure in all recorded motoneurons; second, motoneurons with low recruitment threshold current did not change their recruitment threshold current as compared to the control; and third, motoneurons with high recruitment threshold current showed a decrease in this value with glutamate application.

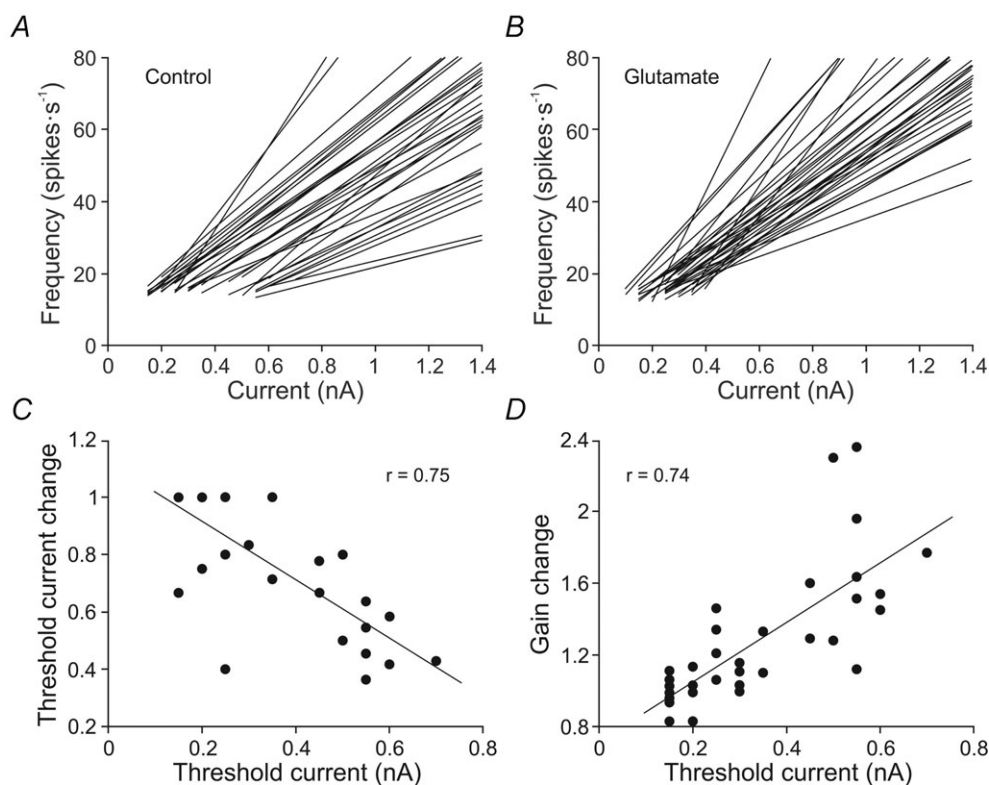


Figure 5. Effect of the glutamate on tonic firing gain and recruitment threshold current

A and B, *I*-*F* plots for all motoneurons in control (A) and glutamate (B) conditions. Note that the range of recruitment threshold current was broader in the control condition. C and D, plots illustrating the change in recruitment threshold current and tonic frequency gain as a function of the recruitment threshold current.

Phasic firing rate response to glutamate exposure

We also quantified the effect of glutamate on the phasic component of the firing rate. With this aim, the peak frequency was calculated in both control and glutamate conditions. Different responses were observed: some motoneurons maintained similar peak frequency in the glutamate condition, while peak frequency increased in other motoneurons. For the motoneuron shown in Fig. 7A, the peak frequency was 47 spikes s^{-1} in the control condition and 70 spikes s^{-1} in the glutamate condition. In the control condition the motoneurons exhibited a peak frequency that ranged from 17.3 to 98.6 spikes s^{-1} (47.7 ± 2.9 spikes s^{-1}), whereas it ranged from 26.6 to 132.3 spikes s^{-1} (58.4 ± 3.5 spikes s^{-1}) in the glutamate condition. The change in peak frequency was different from one motoneuron to another, and it was distributed in a continuum that ranged from 0.6 to 3.3. When change in peak frequency was plotted against recruitment threshold current, a significant linear relationship was found (Fig. 7B). This positive co-variation indicates that the last recruited motoneurons were those whose peak frequency showed a more pronounced increase (up to 3.3-fold) with glutamate exposure. Thus, motoneurons with recruitment

threshold current higher than 0.5 nA exhibited a peak frequency of 52.4 ± 3.7 spikes s^{-1} in control condition, whereas it was 102.6 ± 4.4 spikes s^{-1} when exposed to glutamate. In addition, some motoneurons with low recruitment threshold current exhibited a decrease in peak frequency (between 0.6–1).

Spike frequency adaptation and glutamate

The findings above demonstrate that glutamate treatment modified the tonic and phasic components of firing rate as a function of the recruitment threshold current. The last step was to quantify the spike-frequency adaptation in order to examine if the effect of glutamate on the phasic and tonic firing was similar or, on the contrary, enhanced

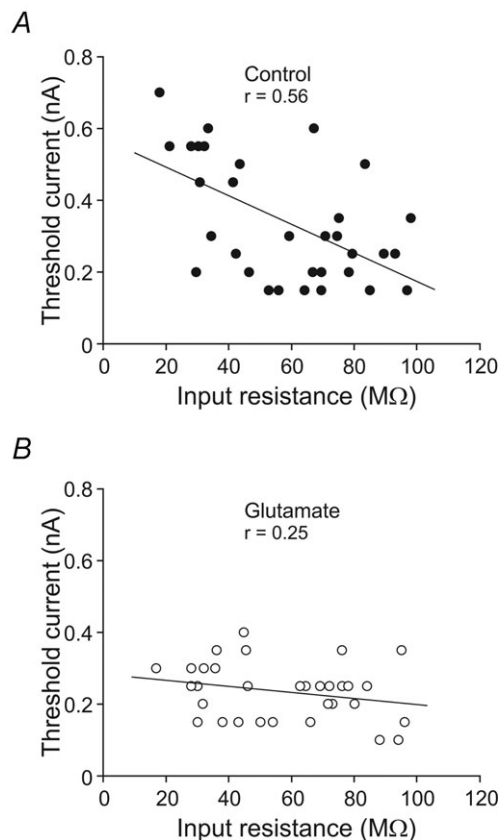


Figure 6. Relationship between input resistance and recruitment threshold current in control (A) and glutamate (B) conditions

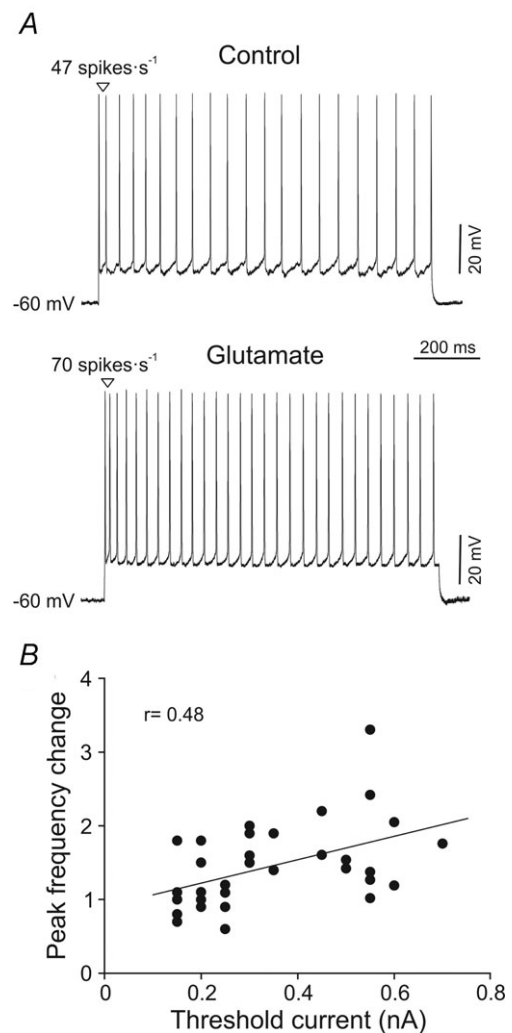


Figure 7. Effect of glutamate on peak frequency. A, a representative high-recruitment threshold current motoneuron recorded in control and glutamate conditions. It should be noted that the first interspike interval was shortened with glutamate. B, plot illustrating the change in peak frequency as a function of the recruitment threshold current.

either the phasic or the tonic component (Fig. 8). The firing patterns of two representative motoneurons are illustrated in Fig. 8A and B. The phasic-tonic firing of the motoneuron shown was almost unaffected in the glutamate condition, whereas the motoneuron documented in Fig. 8B increased its phasic-tonic firing rate in the glutamate condition. The former (Fig. 8A) exhibited peak frequencies (25 vs. 29 spikes s^{-1}) that were close to the steady-state frequency in the control and glutamate conditions (20 vs. 22 spikes s^{-1}). Moreover the glutamate treatment did not produce any observable modification in the discharge patterns. This motoneuron had an adaptation index of 0.20 and 0.24 in control and glutamate conditions, respectively. The peak frequency (47 spikes s^{-1}) of the motoneuron illustrated in Fig. 8B was higher than the steady-state frequency (20 spikes s^{-1}) in the control condition, and glutamate treatment increased both phasic (70 spikes s^{-1}) and tonic (28 spikes s^{-1}) frequencies. This motoneuron exhibited an adaptation index of 0.57 in the control condition and 0.6 with glutamate treatment. Next, we plotted the adaptation

index of all studied motoneurons against recruitment threshold current in control and glutamate conditions (Fig. 8C). The inspection of the raw data in the control condition indicates the following: first, most of the motoneurons (23/33) exhibited an adaptation index between 0.4 and 0.6; second, motoneurons (4/33) with an adaptation index below 0.4 (i.e. with a weak phasic firing component) had recruitment threshold current ≤ 0.2 nA; and third, motoneurons (6/33) with adaptation index up to 0.6 (i.e. with a strong phasic firing component) had recruitment threshold current ≥ 0.35 nA. The comparison of the adaptation index in both control and glutamate conditions showed a significant increase for the whole studied population (control = 0.51 ± 0.02 ; glutamate = 0.55 ± 0.02). Indeed, in most of the motoneurons (26/33) the adaptation index change was higher than 1, whereas it was equal or lower than 1 for a few of them (6/33). In short, glutamate enhanced the phasic component of the firing as compared to the tonic one, and this effect was independent on the recruitment threshold current (Fig. 8D).

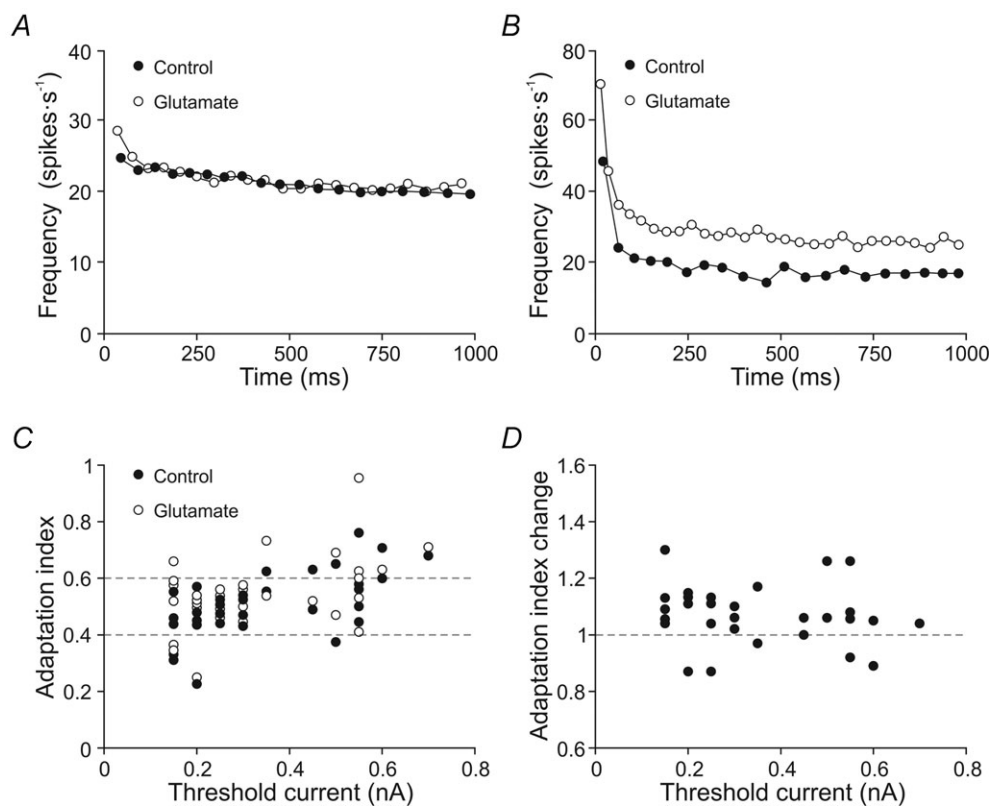


Figure 8. Effect of glutamate on spike frequency adaptation

A and B, plots representing the instantaneous frequency of a low-recruitment threshold current motoneuron (A) and a high-recruitment threshold current motoneuron (B) in control and glutamate conditions. C, plot illustrating the values of initial adaptation index as a function of the recruitment threshold current in control and glutamate conditions. Note most of the motoneurons had adaptation index between 0.4 and 0.6 (grey lines). D, plot illustrating the change in the adaptation index as a function of the recruitment threshold current.

Discussion

Glutamate and current mediated recruitment threshold

This work demonstrates that glutamate modulates the firing properties as a function of recruitment threshold current (and rheobase – data not shown). Both parameters are closely related, but the ratio between rheobase and recruitment threshold current is different among motoneurons. The discrepancy has been attributed to slow membrane non-linearities (Kernell *et al.* 1999). The present work studied the modifications in tonic and phasic firing properties against recruitment threshold current because it resembles more closely the procedure used in the behaving animal to determine the recruitment threshold of the motoneurons. In the behaving animal, the recruitment threshold is interpolated from the relationship between tonic firing rates and eye position (Delgado-Garcia *et al.* 1986; Fuchs *et al.* 1988). As previously reported, the variance is generally low at high firing rates and increases at lower firing rates (Piotrkiewicz, 1999; Powers & Binder, 2000). These authors plotted the standard deviation *versus* the mean of the interspike intervals and described a ‘break point’ interval since they fit with two regression lines for the low- and high-firing variability. The break point provides a relatively crude estimation of spike afterhyperpolarization duration (Powers & Binder, 2000). The minimal steady-state repetitive firing has been shown to be correlated with the reciprocal spike afterhyperpolarization in brainstem (Viana *et al.* 1995; González Forero *et al.* 2002) and spinal cord motoneurons (Kernell, 1965; Powers & Binder, 2000). Our data also support this finding because the mean duration of interspike interval at steady-state firing rate was slightly lower (~ 20 ms) than the duration of single spike afterhyperpolarization previously reported (Carrascal *et al.* 2006; Nieto-Gonzalez *et al.* 2007). Furthermore, estimations of the duration of the spike afterhyperpolarization by studies of firing rate have been carried out in two ways, with the interval histogram transform method (Matthews, 1996) and with the break-point method (Piotrkiewicz *et al.* 1999), and the results are strongly correlated (Zijdewind & Thomas, 2012). These studies provide an effective measure of firing threshold (Powers & Binder, 2000).

The amplitudes of the synaptic input from different systems have been shown to vary systematically in low-*versus* high-threshold spinal motoneurons (Heckman & Binder, 1993*a,b*). As a consequence, motoneuron pools are known to expand or compress the recruitment threshold range. For instance, the activation of homonymous Ia afferents in spinal motoneurons generates a more effective synaptic current in low- rather than high-threshold motoneurons, and produces an expansion

in the recruitment range of motoneurons (Heckman & Binder, 1988); by contrast, synaptic currents from the rubrospinal tract compress the recruitment range by distributing excitation more strongly to motoneurons with intrinsically high thresholds as compared to motoneurons with lower thresholds (Heckman & Binder, 1993*a,b*; Powers *et al.* 1993). In abducens motoneurons, synaptic deprivation of inhibitory or inhibitory plus excitatory inputs due to low and high doses of tetanus neurotoxins, respectively, also modifies the recruitment threshold. The mean recruitment threshold was reduced in both cases, but the opposite effects were observed in the recruitment rank, since it narrowed under low dose and expanded under high dose as compared to the control (Pastor & González-Forero, 2003). Furthermore, vestibular electrical stimulation supports the hypothesis that hyperpolarizing and depolarizing synaptic currents should be more effective in abducens neurons that are recruited later (Broussard *et al.* 1995). These findings demonstrate that the synaptic inputs influence the motoneuron recruitment range. This influence is also present in the oculomotor nucleus motoneurons since the activation of glutamatergic receptors decreased both rheobase and depolarization voltage, and compressed the recruitment threshold current range. These results could be attributable to an increase in input resistance or a decrease in voltage threshold. We rule out input resistance because changes in this parameter did not co-vary with changes in rheobase or depolarization voltage. This finding is consistent with that reported in abducens motoneurons with glutamate application in *in vivo* studies (Durand *et al.* 1987). In addition, it has been reported that the selective activation of different types of glutamatergic receptors decreases (Iwagaki & Miles, 2011), increases (Del Negro & Chandler, 1998; Marchetti *et al.* 2005), or does not modify input resistance (Chapman *et al.* 2008) depending on the studied motoneuron population. In regard to voltage threshold, it has been reported in spinal motoneurons that the activation of group I metabotropic glutamate receptors diminishes the voltage threshold for action potential initiation (Iwagaki & Miles, 2011). The mechanisms underlying the modulation of action potential threshold remains unclear, but potential mechanisms include the modulation of persistent Na^+ currents (Carlier *et al.* 2006) and delayed rectifier K^+ channels (Dai *et al.* 2002).

The order of recruitment of motoneurons has been considered to depend on input resistance, such that small motoneurons with less surface area would have higher input resistance and would produce a larger voltage drop for a given synaptic input than larger ones. Therefore, small motoneurons would also reach voltage threshold at a lower level of synaptic input (Henneman *et al.* 1965; Mendell, 2005). We have recently demonstrated in

oculomotor nucleus motoneurons, first, that the increase in size of motoneurons led to a decrease in input resistance with a strong linear relationship, and second, that an inverse correlation was also found between input resistance and rheobase. According to these findings, the first motoneurons to be recruited are those with small size (Carrascal *et al.* 2011). In alert preparations, the relationship between conduction velocities and the recruitment thresholds of abducens motoneurons was weak in cat and not significant in monkeys or goldfish (Delgado-García *et al.* 1986; Fuchs *et al.* 1988; Pastor *et al.* 1991; Pastor & González-Forero, 2003). These results support the notion that a recruitment order based exclusively on the size principle seems not to be a sufficient criterion for ranking the motoneuronal pool as a function of firing-related parameters (Pastor *et al.* 1991). In this work, the recruitment current range was compressed in high-threshold motoneurons by reduction of voltage threshold. This latter result is consistent with the data previously reported in spinal motoneurons in response to the activation of the rubrospinal input (Powers *et al.* 1993). Assuming that recruitment order depends primarily on cell size, the glutamatergic effects reported here are more pronounced in motoneurons with the largest size. Such a glutamatergic modulation could explain the weak correlation between conduction velocities and recruitment threshold reported in alert preparations.

Glutamate inputs, recruitment threshold and tonic firing

Synaptic inputs can potentially alter the gain of the input–output function of motoneurons (Binder *et al.* 1993; Heckman *et al.* 2003; McElvain *et al.* 2010). The increase in firing rate found in this work could be attributable to the glutamatergic modulation of action potential afterhyperpolarization (Anwyl, 1999; Young *et al.* 2003; Ruiz, 2011). In particular, the activation of group I metabotropic glutamate receptors blocks the voltage-dependent I_M and the Ca^{2+} -activated I_{AHP} (Anwyl, 1999; Young *et al.* 2003). On the other hand, the ocular motoneurons exhibit a tonic discharge which is proportional to eye position, and balances the elastic forces that would otherwise bring the eye back to its primary position (Robinson, 1970). Alert preparation studies have shown that motoneurons begin to fire when the eye position reaches a threshold value in the on-direction. Above this threshold, the firing rate varies linearly with eye position, with a slope k . It is widely accepted that recruitment threshold values and k are related: motoneurons with higher threshold have greater slope k (Delgado-García *et al.* 1986; Fuchs *et al.* 1988; de la Cruz *et al.* 1989). *In vitro*, an inverse relationship

between recruitment current and tonic frequency gain was found, i.e. motoneurons with lower recruitment current have higher gain (Nieto-Gonzalez *et al.* 2007). Assuming that tonic frequency gain mimics k , these results contradict those reported *in vivo*. Therefore, we ruled out intrinsic membrane properties as solely determining the co-variation between recruitment threshold and k reported in alert animals. The negative co-variation between tonic frequency gain and recruitment current found in the control condition using *in vitro* preparation disappear with glutamate treatment. However, we did not obtain a positive co-variation between recruitment threshold current and tonic frequency gain as expected from data in alert preparations. Therefore, glutamatergic inputs in combination with other neurotransmitters and/or trophic factors from the muscle may also be acting to produce the functional positive relationship between motoneuron recruitment threshold and k reported in alert preparations.

Glutamate inputs, recruitment threshold and phasic firing

Ocular motoneurons send a burst of spikes (phasic firing) for executing saccadic eye movements, which is required to overcome the resistance of viscous drag of the orbital tissue (Robinson, 1970). The positive co-variation between the change in peak frequency and recruitment threshold current reported here could contribute to the finding that motoneurons with higher threshold also tend to exhibit higher eye velocity sensitivity (Davis-López de Carrizosa *et al.* 2011). Glutamate exerted a slightly greater increase in the phasic component of the firing rate than in the tonic one. Given that suprathreshold current steps evoke the phasic and tonic components of the firing in oculomotor nucleus motoneurons, it is evident that this firing rate pattern involves the intrinsic active membrane properties of the motoneurons. The conductances underlying such a discharge pattern may be modulated with glutamate, as proposed in other neuron pools (Young *et al.* 2003; Cosgrove *et al.* 2011; Iwagaki & Miles, 2011). On the other hand, it should not be neglected that separate premotor neurons feed the motoneurons with phasic and tonic signals (Scudder *et al.* 2002; Sparks, 2002) and that the phasic and tonic synaptic inputs can be restored independently (Davis-López de Carrizosa *et al.* 2009). Therefore, glutamate may exert a greater influence on the phasic inputs than on the tonic ones.

Functional implications

For the last two decades, there has been a general consensus that the ocular motoneurons discharge pattern was rather homogeneous. All motoneurons have qualitatively similar discharge patterns consisting of phasic firing related

to saccades and tonic firing related to eye position (Delgado-García *et al.* 1986; Fuchs *et al.* 1988; Pastor *et al.* 1991). Recent studies in alert preparations support the view that ocular motoneurons could be classified into continuous overlapping groups of cells, the first group to be recruited being moderately tonic while the last recruited motoneurons are relatively phasic (Davis-López de Carrizosa *et al.* 2011). Additionally, data reported from brain slice preparation in oculomotor and trochlear nuclei have classified motoneurons into a continuum between two canonical types depending on the action-potential shape, spike frequency adaptation, and dynamic range (Nieto-Gonzalez *et al.* 2007, Jones & Ariel, 2008). The present data show that glutamate enhances the phasic–tonic firing as a function of the recruitment threshold current. In conclusion, intrinsic membrane properties, response to excitatory amino acids and functional firing patterns point to the notion that ocular motoneurons are less homogeneous than initially thought.

Motoneuron recruitment threshold and firing rate determine muscle contraction. The present work demonstrates that motoneurons with low-recruitment threshold current have higher input resistance and may be smaller, and exhibit tonic or moderately phasic firing, which remains essentially unmodified by glutamate application. The most tonic motoneurons (i.e. with a weak phasic component) have been proposed to project to non-twitch or multiply innervated fibres that are not suited to significantly contribute to saccadic eye movements, but are more suited to play a role in eye fixation (Büttner-Ennever *et al.* 2001; Eberhorn *et al.* 2005, 2006; Nieto-Gonzalez *et al.* 2007; Davis-López de Carrizosa *et al.* 2011). In contrast, motoneurons with high recruitment threshold current, which have lower input resistance and may be larger, show a phasic–tonic firing whose rate is strengthened by glutamate. These motoneurons could project to twitch or singly innervated fibres (Büttner-Ennever *et al.* 2001) with different contraction speed and fatigability (Nelson *et al.* 1986) and could generate a strong muscle contraction under glutamate modulation to perform saccadic eye movements with different velocities and/or to maintain the eye in different eccentric positions in the orbit.

References

- Anwyl R (1999). Metabotropic glutamate receptors: electrophysiological properties and role in plasticity. *Brain Res Rev* **29**, 83–120.
- Binder MD, Heckman CJ & Powers RK (1993). How different afferent inputs control motoneuron discharge and the output of the motoneuron pool. *Curr Opin Neurobiol* **3**, 1028–1034.
- Broussard DM, DeCharms RC & Lisberger SG (1995). Inputs from the ipsilateral and contralateral vestibular apparatus to behaviorally characterized abducens neurons in rhesus monkeys. *J Neurophysiol* **74**, 2445–2459.
- Büttner-Ennever JA, Horn AK, Scherberger H & D'Ascanio P (2001). Motoneurons of twitch and nontwitch extraocular muscle fibers in the abducens, trochlear, and oculomotor nuclei of monkeys. *J Comp Neurol* **438**, 318–335.
- Carlier E, Sourdet V, Boudkazi S, Déglise P, Ankri N, Fronzaroli-Molinieres L & Debanne D (2006). Metabotropic glutamate receptor subtype 1 regulates sodium currents in rat neocortical pyramidal neurons. *J Physiol* **577**, 141–154.
- Carpenter MB, Periera AB & Guha N (1992). Immunocytochemistry of oculomotor afferents in the squirrel monkey (*Saimiri sciureus*). *J Hirnforsch* **33**, 151–167.
- Carrascal L, Nieto-Gonzalez JL, Nunez-Abades P & Torres B (2006). Temporal sequence of changes in electrophysiological properties of oculomotor motoneurons during postnatal development. *Neuroscience* **140**, 1223–1237.
- Carrascal L, Nieto-Gonzalez JL, Nunez-Abades P & Torres B (2011). Diminution of voltage threshold plays a key role in determining recruitment of oculomotor nucleus motoneurons during postnatal development. *Plos One* **6**, e28748.
- Chapman RJ, Issberner JP & Sillar KT (2008). Group I mGluRs increase locomotor network excitability in *Xenopus* tadpoles via presynaptic inhibition of glycinergic neurotransmission. *Eur J Neurosci* **28**, 903–913.
- Cosgrove KE, Galván EJ, Barrionuevo G & Meriney SD (2011). mGluRs modulate strength and timing of excitatory transmission in hippocampal area CA3. *Mol Neurobiol* **44**, 93–101.
- Davis-López de Carrizosa MA, Morado-Díaz CJ, Miller JM, de la Cruz RR & Pastor AM (2011). Dual encoding of muscle tension and eye position by abducens motoneurons. *J Neurosci* **31**, 2271–2279.
- Davis-López de Carrizosa MA, Morado-Díaz CJ, Tena JJ, Benítez-Temiño B, Pecero ML, Morcuende SR, de la Cruz RR & Pastor AM (2009). Complementary actions of BDNF and neurotrophin-3 on the firing patterns and synaptic composition of motoneurons. *J Neurosci* **29**, 575–587.
- Dai Y, Jones KE, Fedirchuk B, McCrea DA & Jordan LM (2002). A modelling study of locomotion-induced hyperpolarization of voltage threshold in cat lumbar motoneurons. *J Physiol* **544**, 521–536.
- de la Cruz RR, Escudero M & Delgado-García JM (1989). Behaviour of medial rectus motoneurons in the alert cat. *Eur J Neurosci* **1**, 288–295.
- Del Negro CA & Chandler SH (1998). Regulation of intrinsic and synaptic properties of neonatal rat trigeminal motoneurons by metabotropic glutamate receptors. *J Neurosci* **18**, 9216–9226.
- Dean P (1997). Simulated recruitment of medial rectus motoneurons by abducens internuclear neurons: synaptic specificity vs. intrinsic motoneuron properties. *J Neurophysiol* **78**, 1531–1549.
- Delgado-García JM, del Pozo F & Baker R (1986). Behavior of neurons in the abducens nucleus of the alert cat-I. Motoneurons. *Neuroscience* **17**, 929–952.
- Durand J, Engberg I & Tyc-Dumont S (1987). L-Glutamate and N-methyl-D-aspartate actions on membrane potential and conductance of cat abducens motoneurons. *Neurosci Lett* **79**, 295–300.

- Durand J (1991). NMDA actions on rat abducens motoneurons. *Eur J Neurosci* **3**, 621–633.
- Durand J (1993). Synaptic excitation triggers oscillations during NMDA receptor activation in rat abducens motoneurons. *Eur J Neurosci* **5**, 1389–1397.
- Eberhorn AC, Ardeleanu P, Büttner-Ennever JA & Horn AK (2005). Histochemical differences between motoneurons supplying multiply and singly innervated extraocular muscle fibers. *J Comp Neurol* **491**, 352–366.
- Eberhorn AC, Büttner-Ennever JA & Horn AK (2006). Identification of motoneurons supplying multiply- or singly-innervated extraocular muscle fibers in the rat. *Neuroscience* **137**, 891–903.
- Fuchs AF, Scudder CA & Kaneko CR (1988). Discharge patterns and recruitment order of identified motoneurons and internuclear neurons in the monkey abducens nucleus. *J Neurophysiol* **60**, 1874–1895.
- Fuller PI, Reddrop C, Rodger J, Bellingham MC & Phillips JK (2006). Differential expression of the NMDA NR2B receptor subunit in motoneuron populations susceptible and resistant to amyotrophic lateral sclerosis. *Neurosci Lett* **399**, 157–161.
- Gómez C, Torres B, Jimenez-Ridruejo G & Delgado-García JM (1986). A quantitative analysis of abducens motoneuron behavior during saccadic eye movements in the alert cat. *Neurosci Res* **3**, 345–350.
- González-Forero D, Alvarez FJ, de la Cruz RR, Delgado-García JM & Pastor AM (2002). Influence of afferent synaptic innervation on the discharge variability of cat abducens motoneurons. *J Physiol* **541**, 283–299.
- Hazel TR, Sklavos SG & Dean P (2002). Estimation of premotor synaptic drives to simulated abducens motoneurons for control of eye position. *Exp Brain Res* **146**, 184–196.
- Heckman CJ & Binder MD (1988). Analysis of effective synaptic currents generated by homonymous Ia afferent fibers in motoneurons of the cat. *J Neurophysiol* **60**, 1946–1966.
- Heckman CJ & Binder MD (1993a). Computer simulations of the effects of different synaptic input systems on motor unit recruitment. *J Neurophysiol* **70**, 1827–1840.
- Heckman CJ & Binder MD (1993b). Computer simulations of motoneuron firing rate modulation. *Neurophysiol* **69**, 1005–1008.
- Heckman CJ, Lee RH & Brownstone RM (2003). Hyperexcitable dendrites in motoneurons and their neuromodulatory control during motor behavior. *Trends Neurosci* **26**, 688–695.
- Henneman E, Somjen G & Carpenter DO (1965). Functional significance of cell size in spinal motoneurons. *J Neurophysiol* **28**, 560–580.
- Hideyama T, Yamashita T, Suzuki T, Tsuji S, Higuchi M, Seeburg PH, Takahashi R, Misawa H & Kwak S (2010). Induced loss of ADAR2 engenders slow death of motor neurons from Q/R site-unedited GluR2. *J Neurosci* **30**, 11917–11925.
- Iwagaki N & Miles GB (2011). Activation of group I metabotropic glutamate receptors modulates locomotor-related motoneuron output in mice. *J Neurophysiol* **105**, 2108–2120.
- Jones MS & Ariel M (2008). Morphology, intrinsic membrane properties, and rotation-evoked responses of trochlear motoneurons in the turtle. *J Neurophysiol* **99**, 1187–1200.
- Kernell D (1965). The limits of firing frequency in cat lumbosacral motoneurons possessing different time course of afterhyperpolarization. *Acta Physiol Scand* **65**, 87–100.
- Kernell D, Bakels R & Copray JC (1999). Discharge properties of motoneurons: how are they matched to the properties and use of their muscle units? *J Physiol Paris* **93**, 87–96.
- Kevetter GA & Hoffman RD (1991). Excitatory amino acid immunoreactivity in vestibulo-ocular neurons in gerbils. *Brain Res* **554**, 348–351.
- Laslo P, Lipski J & Funk GD (2001a). Differential expression of Group I metabotropic glutamate receptors in motoneurons at low and high risk for degeneration in ALS. *Neuroreport* **12**, 1903–1908.
- Laslo P, Lipski J, Nicholson LF, Miles GB & Funk GD (2001b). GluR2 AMPA receptor subunit expression in motoneurons at low and high risk for degeneration in amyotrophic lateral sclerosis. *Exp Neurol* **169**, 461–471.
- Marchetti C, Taccola G & Nistri A (2005). Activation of group I metabotropic glutamate receptors depresses recurrent inhibition of motoneurons in the neonatal rat spinal cord in vitro. *Exp Brain Res* **164**, 406–410.
- Matthews PB (1996). Relationship of firing intervals of human motor units to the trajectory of post-spike after-hyperpolarization and synaptic noise. *J Physiol* **492**, 597–628.
- McElvain LC, Bagnall MW, Sakatos A & du Lac S (2010). Bidirectional plasticity gated by hyperpolarization control of gain of postsynaptic firing responses at central vestibular nerve synapses. *Neuron* **68**, 763–775.
- Mendell LM (2005). The size principle: a rule describing the recruitment of motoneurons. *J Neurophysiol* **93**, 3024–3026.
- Nelson JS, Goldberg SJ & McClung JR (1986). Motoneuron electrophysiological and muscle contractile properties of superior oblique motor units in cat. *J Neurophysiol* **55**, 715–726.
- Nguyen LT, Baker R & Spencer RF (1999). Abducens internuclear and ascending tract of Deiters inputs to medial rectus motoneurons in the cat oculomotor nucleus: synaptic organization. *J Comp Neurol* **405**, 141–159.
- Nguyen LT & Spencer RF (1999). Abducens internuclear and ascending tract of Deiters inputs to medial rectus motoneurons in the cat oculomotor nucleus: neurotransmitters. *J Comp Neurol* **411**, 73–86.
- Nieto-Gonzalez JL, Carrascal L, Nunez-Abades PA & Torres B (2007). Phasic and tonic firing properties in rat oculomotor nucleus motoneurons, studied in vitro. *Eur J Neurosci* **25**, 2682–2696.
- Nieto-Gonzalez JL, Carrascal L, Nunez-Abades P & Torres B (2009). Muscarinic modulation of recruitment threshold and firing rate in rat oculomotor nucleus motoneurons. *J Neurophysiol* **101**, 100–111.
- Ouardouz M & Durand J (1994). Involvement of AMPA receptors in trigeminal post-synaptic potentials recorded in rat abducens motoneurons in vivo. *Eur J Neurosci* **6**, 1662–1668.

- Pastor AM & González-Forero D (2003). Recruitment order of cat abducens motoneurons and internuclear neurons. *J Neurophysiol* **90**, 2240–2252.
- Pastor AM, Torres B, Delgado-García JM & Baker R (1991). Discharge characteristics of medial rectus and abducens motoneurons in the goldfish. *J Neurophysiol* **66**, 2125–2140.
- Piotrkiewicz M (1999). An influence of afterhyperpolarization on the pattern of motoneuronal rhythmic activity. *J Physiol Paris* **93**, 125–133.
- Powers RK & Binder MD (2000). Relationship between the time course of the afterhyperpolarization and discharge variability in cat spinal motoneurons. *J Physiol* **528**, 131–150.
- Powers RK, Robinson FR, Konodi MA & Binder MD (1993). Distribution of rubrospinal synaptic input to cat triceps surae motoneurons. *J Neurophysiol* **70**, 1460–1468.
- Rekling JC, Funk GD, Bayliss DA, Dong XW & Feldman JL (2000). Synaptic control of motoneuronal excitability. *Physiol Rev* **80**, 767–852.
- Robinson, DA (1970). Oculomotor unit behavior in the monkey. *J Neurophysiol* **33**, 393–403.
- Ruiz A & Durand J (1999). Modulation of kainate-induced responses by pentobarbitone and GYKI-53784 in rat abducens motoneurons in vivo. *Brain Res* **818**, 421–430.
- Ruiz A (2011). Kainate receptors with a metabotropic signature enhance hippocampal excitability by regulating the slow after-hyperpolarization in CA3 pyramidal neurons. *Adv Exp Med Biol* **717**, 59–68.
- Sawczuk A, Powers RK & Binder MD (1995). Spike frequency adaptation studied in hypoglossal motoneurons of the rat. *J Neurophysiol* **73**, 1799–1810.
- Scudder CA, Kaneko CS & Fuchs AF (2002). The brainstem burst generator for saccadic eye movements: a modern synthesis. *Exp Brain Res* **142**, 439–462.
- Sparks DL (2002). The brainstem control of saccadic eye movements. *Nat Rev Neurosci* **3**, 952–964.
- Spencer RF & Wang SF (1996). Immunohistochemical localization of neurotransmitters utilized by neurons in the rostral interstitial nucleus of the medial longitudinal fasciculus (riMLF) that project to the oculomotor and trochlear nuclei in the cat. *J Comp Neurol* **366**, 134–148.
- Stahl JS & Simpson JI (1995). Dynamics of abducens nucleus neurons in the awake rabbit. *J Neurophysiol* **73**, 1383–1395.
- Sylvestre PA & Cullen KE (1999). Quantitative analysis of abducens neuron discharge dynamics during saccadic and slow eye movements. *J Neurophysiol* **82**, 2612–2632.
- Viana F, Bayliss DA & Berger AJ (1995). Repetitive firing properties of developing rat brainstem motoneurons. *J Physiol* **486**, 745–761.
- Young SR, Chuang SC & Wong RK (2003). Modulation of afterpotentials and firing pattern in guinea pig CA3 neurones by group I metabotropic glutamate receptors. *J Physiol* **554**, 371–385.
- Zijdewind I & Thomas CK (2012). Firing patterns of spontaneously active motor units in spinal cord-injured subjects. *J Physiol* **590**, 1683–1697.

Author contributions

J.T.-T., D.R.-R. and L.C. carried out the collection and analysis of the data. P.N.-A., L.C. and B.T. participated in the conception and design of the experiments. All authors drafted the article.

Acknowledgements

We wish to thank Drs Germán Barrionuevo (University of Pittsburgh), Laurent Goffart (Institut de Neurosciences de la Timone, Aix-Marseille Universités), María A. Davis-López de Carrizosa and Ángel M. Pastor (University of Seville) for their suggestions and critical reading of a previous version of the manuscript. We thank Ms Anna Rose Thomas for her help in the revision of the English manuscript. This work was supported by a grant from the Ministerio de Ciencia y Tecnología (BFU 2009-07867) and Proyectos de Excelencia de la Junta de Andalucía (P08-CVI-039 and P09-CVI-4617).